BIOENGINEERING

Vasculogenic hydrogel enhances islet survival, engraftment, and function in leading extrahepatic sites

Jessica D. Weaver,[1,2] Devon M. Headen,[1,2] Jahizreal Aquart,[2] Christopher T. Johnson,[2,3] Lonnie D. Shea,[4,5] Haval Shirwan,[6,7] Andrés J. García[1,2]*

Islet transplantation is a promising alternative therapy for insulin-dependent patients, with the potential to eliminate life-threatening hypoglycemic episodes and secondary complications of long-term diabetes. However, widespread application of this therapy has been limited by inadequate graft function and longevity, in part due to the loss of up to 60% of the graft in the hostile intrahepatic transplant site. We report a proteolytically degradable synthetic hydrogel, functionalized with vasculogenic factors for localized delivery, engineered to deliver islet grafts to extrahepatic transplant sites via in situ gelation under physiological conditions. Hydrogels induced differences in vascularization and innate immune responses among subcutaneous, small bowel mesentery, and epididymal fat pad transplant sites with improved vascularization and reduced inflammation at the epididymal fat pad site. This biomaterial-based strategy improved the survival, engraftment, and function of a single pancreatic donor islet mass graft compared to the current clinical intraportal delivery technique. This biomaterial strategy has the potential to improve clinical outcomes in islet autotransplantation after pancreatectomy and reduce the burden on donor organ availability by maximizing graft survival in clinical islet transplantation for type 1 diabetes patients.

INTRODUCTION

Type 1 diabetes mellitus, a chronic condition characterized by the autoimmune destruction of pancreatic islets and an inability to regulate blood glucose, affects millions of patients worldwide (*1*). Exogenous insulin administration does not accurately recapitulate normal glucose dynamics, and diabetic patients face recurrent and life-threatening hypoglycemic episodes and serious secondary complications, such as retinopathy, neuropathy, and nephropathy (*2*). Islet transplantation is a promising cell therapy for the treatment of type 1 diabetes mellitus, with the potential to restore normal blood glucose regulation and eliminate secondary complications (*3*). Clinical trials with intrahepatic allogeneic islet transplantation have demonstrated insulin independence in diabetic patients, but the median duration of insulin independence is only 35 months and requires multiple donor pancreata (*4*). Although clinically accessible for islet delivery, the hepatic vasculature is an inhospitable transplant site, as evidenced by suboptimal performance of grafts in islet autotransplantation after total pancreatectomy (*5*, *6*). Instant blood-mediated inflammatory responses to intraportally infused islets contribute to rapid graft destruction (*7*–*9*), resulting in an immediate loss of 50 to 60% of the graft (*10*), a substantial barrier to the translation of this therapy. Further graft destruction is mediated by both innate and acquired immune responses, even with chronic immunosuppressive regimens (*11*).

Various extrahepatic transplant sites have been explored to avoid instant blood-mediated inflammatory response–instigated graft loss, including the subcutaneous (SUBQ) space (*12*–*16*) and laparoscopically accessible intraperitoneal locations, such as the small bowel mesentery (SBM) (*17*, *18*) and omentum (*19*–*22*) or the murine omentum equivalent, the epididymal fat pad (EFP) (*23*–*25*). Although the accessibility of these extrahepatic sites is appealing, these tissues present varying degrees of vascular supply and inflammatory responses, which influence islet survival, engraftment, and function (*26*–*28*). Preclinical models using intraportal, renal subcapsular, or splenic subcapsular transplant sites have demonstrated that reestablishment of blood flow to islets requires days to weeks (*29*–*31*), resulting in ischemic conditions during the revascularization period and a vascular bed with lower vessel density and oxygen tension than in the native pancreas (*32*, *33*). This inadequate revascularization of transplanted islets is a major cause of reduced islet viability, function, and engraftment (*34*–*36*). Delivery of provascularization factors via genetic manipulation of islets or biomaterials has shown improved vascularization and islet function (*24*, *37*–*42*). However, these strategies are hindered by suboptimal pharmacokinetics, inadequate delivery matrices, and technical and safety considerations, and evaluate impracticably large islet masses in a limited diversity of sites.

Here, we report a synthetic hydrogel vehicle engineered to enhance extrahepatic site vascularization. We evaluate the impact of this vasculogenic hydrogel on islet engraftment and function in three extrahepatic sites: SUBQ, SBM, and EFP. This versatile hydrogel facilitates minimally invasive and facile cell delivery to extrahepatic sites and enhances islet survival compared to the suboptimal clinical intrahepatic site. Furthermore, this biomaterial-based strategy enables the restoration of euglycemia via the islet yield from a single pancreatic donor, which is a clinical limitation in diabetes reversal due to limited donor availability and increased rejection risk posed by multiple donors, suggesting that its implementation could improve clinical outcomes in islet autotransplantation after total pancreatectomy and reduce the burden on donor organ availability in clinical islet transplantation for type 1 diabetes mellitus patients.

[1]Woodruff School of Mechanical Engineering, Georgia Institute of Technology, Atlanta, GA, 30332, USA. [2]Petit Institute for Bioengineering and Bioscience, Georgia Institute of Technology, Atlanta, GA, 30332, USA. [3]Coulter Department of Biomedical Engineering, Georgia Tech and Emory University, Atlanta, GA, 30332, USA. [4]Department of Biomedical Engineering and Department of Chemical Engineering, University of Michigan, Ann Arbor, MI, 48109, USA. [5]Department of Obstetrics and Gynecology, Feinberg School of Medicine, Northwestern University, Suite 03-2303, 250 East Superior Street, Chicago, IL 60611, USA. [6]Institute of Cellular Therapeutics, Department of Microbiology and Immunology, University of Louisville School of Medicine, Louisville, KY, 40202, USA. [7]FasCure Therapeutics LLC, 300 East Market Street, Louisville, KY 40202, USA.
*Corresponding author. Email: andres.garcia@me.gatech.edu

RESULTS

Localized vascular endothelial growth factor delivery via synthetic hydrogel induces vascularization to different degrees among extrahepatic transplant sites

We explored the ability of a synthetic hydrogel to promote localized vascularization in extrahepatic transplant sites via controlled delivery of vascular endothelial growth factor (VEGF) (Fig. 1). This poly(ethylene glycol) (PEG) hydrogel consists of maleimide-functionalized, four-arm macromers cross-linked into a network using protease-degradable peptides (*17*, *43*). The hydrogel is functionalized with RGD adhesive peptide to promote cell adhesion and ingrowth; VEGF is tethered into the hydrogel network and released in a sustained, on-demand fashion, as infiltrating host cells remodel the gel via proteolytic degradation within a 2- to 4-week period (*17*). VEGF-containing (PEG-VEGF) and control (PEG) hydrogels (50 μl) were polymerized in situ within the SUBQ space or onto SBM or EFP tissue in C57BL/6J recipient mice (fig. S1). Two or 4 weeks after implantation, mice were perfused with fluorescently labeled lectin to identify functional vasculature. Explanted grafts were whole mount–imaged using confocal microscopy (Fig. 2A); the pancreas, liver, and kidney were imaged for reference to native tissue, the current clinical site, and a common preclinical implant site, respectively. Several parameters characterizing the resulting vascularization were evaluated for PEG-VEGF (purple box plot) and control PEG hydrogels (blue box plot) at weeks 2 (open box plots) and 4 (filled box plots) (Fig. 2, B to E) and compared to pancreatic vasculature (dashed line). Differences in vascularization responses to PEG-VEGF hydrogels were observed among alternative transplant sites, particularly by the fractional area metric (Fig. 2B and table S1). By week 4, the SUBQ site exhibited minimal vascularization compared to the pancreas reference ($P < 0.002$ and $P < 0.01$ for PEG and PEG-VEGF, respectively), and vascularization at this site was relatively insensitive to VEGF delivery; the SBM site had comparable vessel fractional area to the pancreas reference for PEG-VEGF groups and little evident improvement over PEG within the same site. Notably, by week 4, PEG-VEGF hydrogels delivered to the EFP enhanced vascularization fractional area, total branch length, junction number, and branch number to significantly greater levels than the SUBQ/PEG-VEGF site (table S1). Together, this analysis demonstrates transplant site–dependent differences in vasculogenesis in response to VEGF-delivering synthetic hydrogels.

Extrahepatic sites exhibit varying leukocyte densities in response to synthetic gels

We examined transplant site inflammatory cell densities 4 weeks after hydrogel delivery as site-specific innate immune responses may influence islet engraftment and survival (*44*). PEG-VEGF and control PEG hydrogels were delivered to the three transplant sites, and inflammatory cell recruitment was evaluated by immunostaining (Fig. 3A). Significant differences in CD45-positive leukocyte percent area were observed among extrahepatic transplant sites (Fig. 3B and table S2), with high leukocyte presence in the SUBQ site (2.0 and 1.1% for PEG and PEG-VEGF, respectively) and decreasing densities for SBM (0.3% for both PEG and PEG-VEGF) and EFP sites (0.2 and 0.03% for PEG and PEG-VEGF, respectively), with the SUBQ site exhibiting an 80-fold ($P < 0.001$) and 40-fold higher ($P < 0.05$) leukocyte expression than EFP/PEG-VEGF for PEG and PEG-VEGF groups, respectively. This trend was also observed for the leukocyte myeloid marker CD11b. These site-specific differences in inflammatory cell recruitment are inversely proportional, by linear nonparametric correlation, to the trends in vascular fractional area for both CD11b ($P = 0.0583$) and CD45 ($P = 0.0167$) markers (fig. S2), where PEG-VEGF recipient sites exhibited reduced resident leukocyte density over PEG controls. Overall, these results show transplant site–dependent responses to vasculogenic hydrogels, with the EFP site demonstrating the lowest degree of inflammatory cell recruitment and equivalent levels of vascularization as native pancreatic tissue.

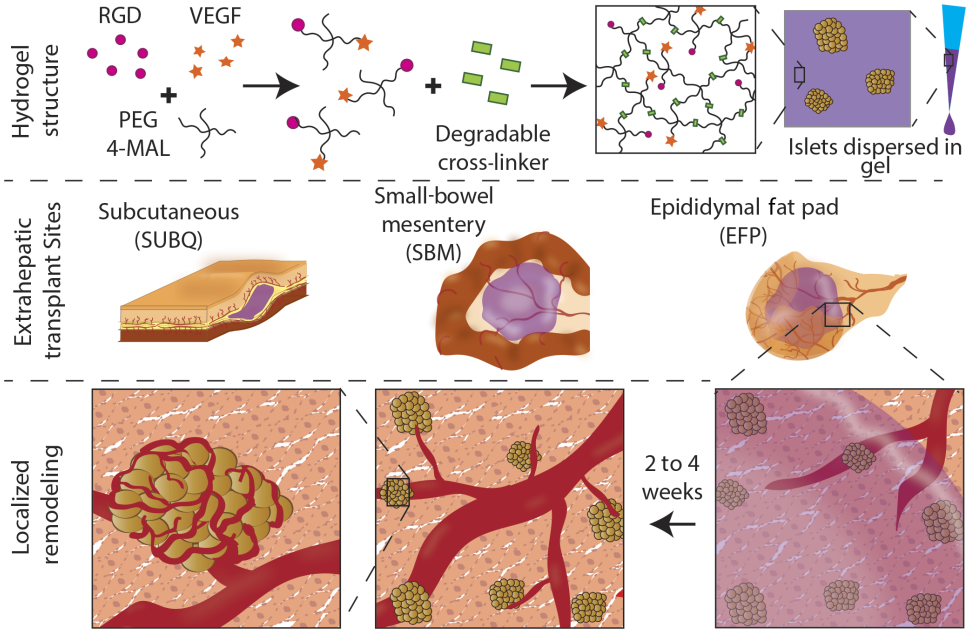

Fig. 1. Schematic demonstrating vasculogenic, proteolytically degradable synthetic hydrogel structure, islet delivery strategy, and localized gel remodeling within extrahepatic transplant sites.

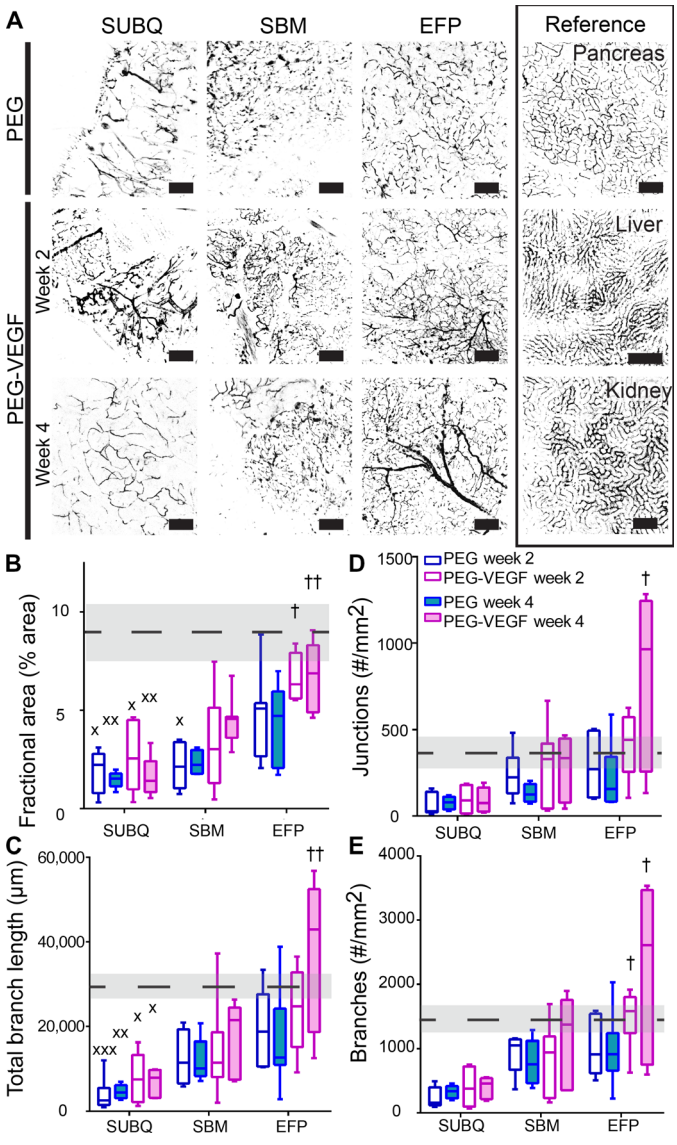

Fig. 2. Localized VEGF enhances vascularization in extrahepatic transplant sites. (**A**) Recipients of PEG-only or VEGF-presenting hydrogels were lectin-perfused at 2 or 4 weeks, and excised grafts were whole mount–imaged. Scale bars, 200 μm. Vascular characteristics of blood vessel fractional area (**B**), total branch length (**C**), junction number (**D**), and branch number per field of view (FOV) (**E**). Dashed line and shaded region represent average and SEM for pancreas reference, respectively. Minimum to maximum box-and-whisker plots, $n = 5$ to 7 per group. † versus SUBQ within the same time point ($^{††}P < 0.01$ and $^{†}P < 0.05$); × versus pancreas control ($^{×××}P < 0.001$, $^{××}P < 0.01$, and $^{×}P < 0.05$); evaluated by Kruskal-Wallis nonparametric tests with Dunn's multiple comparison.

VEGF hydrogel enhances islet engraftment and function in extrahepatic sites

We next examined the effects of vasculogenic hydrogels on the engraftment and function of a single pancreatic donor islet mass in extrahepatic transplant sites, a clinical limitation for diabetes reversal in islet autotransplantation after pancreatectomy and clinical islet transplantation for type 1 diabetes mellitus. We delivered 600 syngeneic islet equivalents (IEQs), the yield from a single C57BL/6J donor mouse, to the SUBQ, SBM, and EFP sites in streptozotocin-induced diabetic mice using PEG-VEGF and control PEG hydrogels. Nonfasting blood glucose (Fig. 4A) was continuously monitored for 5 weeks. Blood glucose values stabilized in most of the individuals by day 15 postoperatively (fig. S3). Average blood glucose levels for islets transplanted with PEG-VEGF to EFP (EFP/PEG-VEGF) were significantly lower than those for islets delivered to SUBQ and SBM using VEGF hydrogels ($P < 0.0001$ and $P < 0.005$ for SUBQ/PEG-VEGF and SBM/PEG-VEGF, respectively) (Fig. 4A). A separate study demonstrated stable, long-term euglycemia out to 100 days for islets delivered to EFP with PEG-VEGF gels (fig. S4A), and islet graft removal ($n = 1$) resulted in a return to hyperglycemia, confirming islet graft–dependent function. Additionally, robust insulin staining and proximal CD31-positive blood vessels (fig. S4, B and C) further confirmed long-term EFP/PEG-VEGF islet engraftment and function. Islets transplanted via hydrogel to the EFP outperformed islets transplanted into SUBQ and SBM sites, with 60 and 75% diabetes reversal within 30 days for EFP/PEG and EFP/PEG-VEGF groups, respectively (Fig. 4C), compared to 0% in the same period for intrahepatic controls (fig. S5, A and B). An intraperitoneal glucose tolerance test (IPGTT) evaluated graft responsiveness to bolus glucose 35 days after transplantation (Fig. 4D). Islets delivered via PEG-VEGF and PEG control hydrogels to EFP and SBM sites performed similarly to glucose bolus, indicating sufficient islet engraftment to respond to a single glucose challenge, whereas subjects receiving islets in PEG-VEGF to the SUBQ site exhibited minimal glucose responsiveness, evidencing limited islet engraftment. An insufficient number of SUBQ/PEG subjects survived to the 35-day time point to include in IPGTT and body weight analysis (fig. S6). Subject body weight was monitored continuously for the duration of the study as an additional metric of graft performance (Fig. 4E), and only the SUBQ/PEG-VEGF group exhibited substantial weight loss (5%) by the end point, further illustrating the poorest islet engraftment in this site among all groups.

To examine functional vascular remodeling of islet grafts delivered with hydrogels, we perfused subjects with labeled lectin at the end point of the study, and whole-mount graft imaging enabled three-dimensional (3D) visualization of functional vasculature (green) and insulin-positive (magenta) transplanted islets (Fig. 4F). Engrafted islets were easily locatable, as the islet organoid vasculature presents as a tight, organized, glomerular-like grouping of dense, lectin-positive blood vessels. The observed density of engrafted islets varied between extrahepatic transplant sites, where the EFP site exhibited numerous vascularized islets, the SBM site displayed intermediate numbers of vascularized islets, and very few vascularized islets were observed in the SUBQ site (fig. S7). Notably, insulin staining for grafts excised at day 35 was exclusively limited to vascularized islets, and no lectin-negative islets were observed. In addition, a higher density of vascularized islets was observed for PEG-VEGF gels, especially for the EFP site (fig. S7). Finally, analysis of normoglycemic subjects transplanted with islets in the EFP via PEG-VEGF gels also showed vascularized islets 100 days after transplantation (fig. S4C). These patterns of islet engraftment and vascularization mirror the functional performance of the grafts, indicating that islet survival, engraftment, and functionality are dependent on integration with transplant site vasculature.

The SUBQ/PEG group experienced the poorest survival ($P < 0.05$; fig. S6), due to hypoglycemic events occurring within the first week after transplant, which may be partly attributable to an elevated innate immune response and corresponding acute loss of transplanted islets, resulting in rapid insulin release, also referred to as insulin "dumping" (Figs. 3 and 4) (*45*). Together, these results demonstrate transplant site–specific differences in vascularization and inflammatory responses

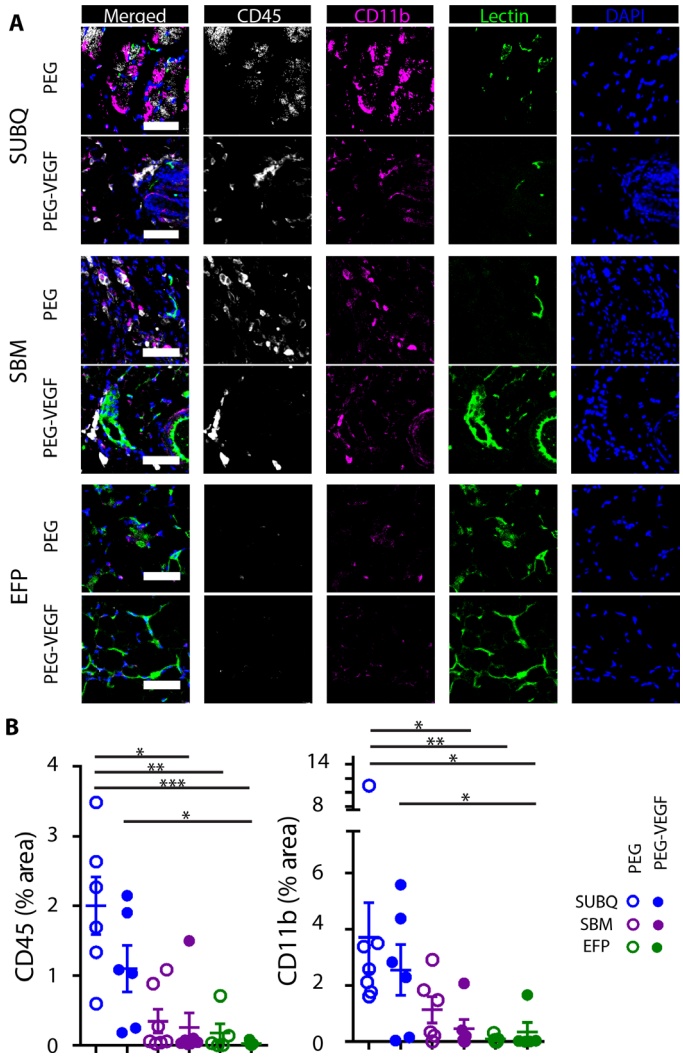

Fig. 3. Leukocyte density varies within extrahepatic transplant sites 4 weeks after hydrogel transplantation. (**A**) Extrahepatic transplant site tissue explanted at week 4 after implantation was stained for CD45 (white) and CD11b (magenta) and was imaged for functional vasculature [lectin (green)] and cell nuclei [DAPI (4′,6-diamidino-2-phenylindole) (blue)]. Scale bars, 50 μm. (**B**) CD11b and CD45 staining was quantified and normalized to FOV area. $n = 4$ to 7 subjects per group. $^{*}P < 0.05$, $^{**}P < 0.01$, and $^{***}P < 0.001$, evaluated by Kruskal-Wallis nonparametric tests with Dunn's multiple comparison.

to the hydrogel vehicle and a strong correlation between these responses and islet graft function. Hydrogel-based delivery of a single pancreatic donor mass of islets to the EFP via PEG-VEGF gels resulted in the most consistent and accelerated return to euglycemia in this nonfasting murine diabetic model.

In vivo tracking demonstrates vasculogenic hydrogel–dependent islet survival in extrahepatic sites

The immediate loss of a large proportion of donor islets during intrahepatic infusion requires multiple donors per recipient and presents a significant barrier to the effective and widespread application of islet replacement therapy (*34*, *46*). To directly assess transplanted islet survival in extrahepatic sites following hydrogel-based delivery, we transplanted islets constitutively expressing luciferase (Luc) and green fluorescent protein (GFP) using PEG hydrogels to the SUBQ and EFP sites and tracked them over time using in vivo bioluminescent imaging. NOD-SCID (nonobese diabetic–severe combined immunodeficient) recipients were chosen to prevent immune rejection of $Luc^{+}GFP^{+}$ islets from a C57BL/6J;FVB background. Pilot studies with various ratios of $Luc^{+}GFP^{+}$/unlabeled islets (a total of 600 IEQs) in immunocompetent C57BL/6J (B6) recipients determined that an optimal loading of 200-IEQ $Luc^{+}GFP^{+}$ islets provided sufficient signal to track islet graft survival and loss and confirmed the expected loss in luminescence signal upon immune rejection beginning 21 days after transplantation (fig. S8). To replicate the graft conditions of our syngeneic studies, 400-IEQ B6 islets were codelivered with 200-IEQ $Luc^{+}GFP^{+}$ islets to achieve a single pancreatic donor islet mass of 600 IEQs. The islets were delivered to extrahepatic sites in PEG-VEGF or control PEG hydrogels and imaged weekly following intraperitoneal luciferin injection (Fig. 5A). An intrahepatic control group was included to compare extrahepatic hydrogel delivery against the clinical standard for islet transplantation, where islets are infused through the portal vein via a saline solution and become entrapped in hepatic vasculature. Because of the possibility of thrombosis and loss of blood flow within the liver upon injection of hydrogel within the vasculature, no PEG or PEG-VEGF was delivered to the intraportal reference site.

Within 1 week after transplant, we observed a moderate increase in luciferase signal of $Luc^{+}GFP^{+}$ islets delivered to the EFP via PEG-VEGF (Fig. 5, B and C), and the signal remained elevated throughout the 35-day imaging window. The signal increase over day 0 readings is attributed to improved metabolic activity of islets after integration with host vasculature (see below). For islets delivered to the EFP using control PEG hydrogel, the luciferase signal remained constant over time but was twofold lower than the corresponding signal from islets delivered using PEG-VEGF hydrogel ($P < 0.01$; Fig. 5C). Islets delivered to the SUBQ site using PEG-VEGF hydrogel displayed a 16-fold lower signal than EFP/PEG at early time points and a 6-fold lower signal at later time points. Finally, islets transplanted in SUBQ using control gel showed loss in bioluminescence signal over time, reaching background levels after 21 days. Overall, the PEG-VEGF hydrogel vehicle enhanced islet bioluminescence signal compared to the control hydrogel for both transplant sites, and the EFP/PEG-VEGF group showed higher and sustained bioluminescence signal compared to all other groups (Fig. 5C), demonstrating that delivery of islets to EFP via PEG-VEGF provides superior islet survival compared to hydrogel control vehicle and other extrahepatic sites. To further support that this effect is because of improved islet integration, we perfused subjects with labeled lectin at day 35 to examine $Luc^{+}GFP^{+}$/B6 islet vascularization (Fig. 5D). Consistent with the syngeneic study, a high density of well-vascularized B6 (GFP-negative) and $Luc^{+}GFP^{+}$ islets was observed for islets transplanted into the EFP with PEG-VEGF. In contrast, fewer and poorly vascularized islets were detected in the SUBQ site.

We observed poor bioluminescence signal from intraportally infused islets (Fig. 5C), with a rapid loss in signal by week 2 after infusion. As with extrahepatic sites, an increase in signal was observed at week 1 after infusion and is likely due to a period of improved metabolic activity (fig. S9A). This rapid loss in bioluminescence signal is consistent with the well-documented instant blood-mediated inflammatory response–instigated intrahepatic islet graft destruction (*46*) and highlights the significant advantage of extrahepatic sites over intraportal delivery for islet survival. Intrahepatic islet loss was confirmed by whole-mount imaging of lectin and GFP at week 6 after infusion (fig. S9B), where only small, fragmented islets were found within the hepatic vasculature.

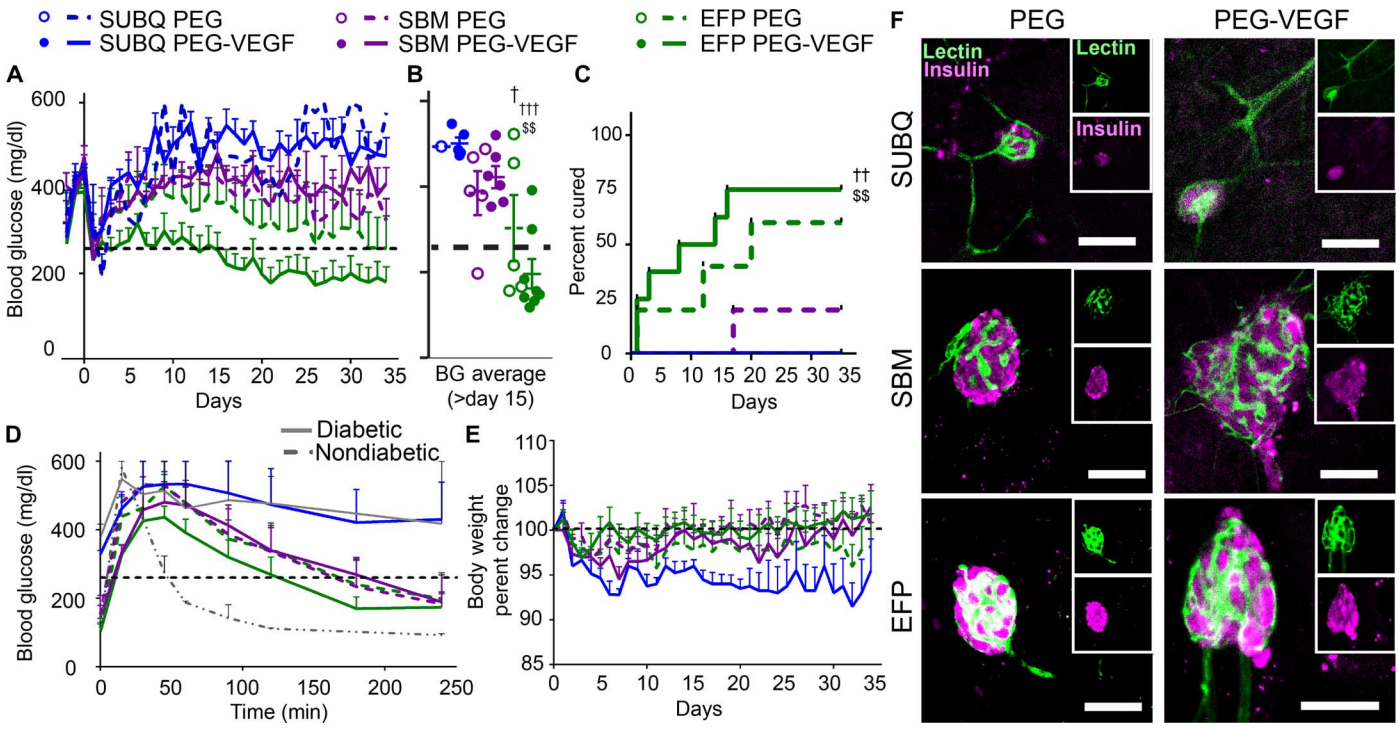

Fig. 4. Vasculogenic hydrogels promote engraftment and function of single pancreatic donor islet graft. Gels containing islets, either with or without VEGF, were delivered to extrahepatic sites. (**A**) Recipients were monitored daily for nonfasting blood glucose values for calculation of average blood glucose (beyond postoperative day 15) (**B**) and survival curve of diabetes reversal (**C**). Graft function was further evaluated by IPGTT on day 35 (**D**) and by monitoring of recipient body weight (**E**). (**F**) Whole-mount imaging of lectin (green)–perfused grafts enabled 3D visualization of engrafted islet vascular network. Error bars represent SEM. Scale bars, 100 μm. $n = 5$ to 8 per group. † versus SUBQ ($^{†††}P < 0.001$, $^{††}P < 0.01$, and $^{†}P < 0.05$); $ versus SBM within the same group (control or VEGF) ($^{\$\$}P < 0.01$). Blood glucose averages were evaluated by one-way analysis of variance (ANOVA), and survival curve analysis was performed using log-rank (Mantel-Cox) test.

We also analyzed the time-to-peak bioluminescence signal after luciferin injection for each imaging time point (Fig. 5E and fig. S10). The rate of bioluminescence signal production serves as an indirect metric of islet vascularization as faster bioluminescence signal kinetics can be attributed to greater islet integration with host vasculature. The EFP/PEG and EFP/PEG-VEGF groups showed a comparable decrease in time-to-peak signal to stable values within 7 days after transplant, suggesting establishment of islet vascularization within this time frame. The SUBQ/PEG-VEGF group decreased to a stable time-to-peak signal by week 2, whereas the SUBQ/PEG group maintained an elevated time-to-peak signal until week 5, providing further evidence that localized VEGF delivery accelerates and enhances site vascularization. Additionally, poor SUBQ site vascularization and subsequent luciferin transport kinetics may explain the 16-fold lower bioluminescence signal observed on day 0. As expected, intraportally infused islets demonstrated rapid times to bioluminescence signal peak throughout the study period due to direct exposure to systemic blood supply within the hepatic vasculature. The EFP/PEG, EFP/PEG-VEGF, and intraportal group demonstrated consistent reduced time-to-peak signal through the study period, significantly less than SUBQ/PEG ($P < 0.05$, $P < 0.005$, and $P < 0.001$, respectively), further evidencing superior islet vascularization within the EFP.

DISCUSSION

Here, we investigated the potential of three extrahepatic sites to sustain islet engraftment and function when delivered in a synthetic hydrogel carrier with or without VEGF and to improve graft survival over the current clinical technique. Although the islet transplantation field broadly recognizes that intrahepatic islet delivery is incompatible with establishing consistent insulin independence, there is a lack of consensus on the optimal extrahepatic site (*21*). A unique advantage of this hydrogel platform is the capacity to directly evaluate leading extrahepatic sites in parallel, and the use of a clinically relevant islet loading shows the feasibility of these sites for translation.

The SUBQ site has been repeatedly explored because it is readily accessible, potentially retrievable, and minimally invasive (*12*, *13*, *15*). However, the low degree of vascularization and heightened immune response in the SUBQ space demonstrated here and in a previous study (*13*) indicate that the SUBQ site is poorly suited for islet engraftment. Whereas the use of the SUBQ site is ubiquitous for the evaluation of vascularization strategies for tissue engineering applications, it is evident that the suitability of this site is application- and context-dependent. The SBM has a large, vascularized surface area to potentially accommodate large transplant volumes; however, this site is not readily retrievable without disturbance of the bowel, and the open nature of the site lends itself to potential islet loss into the peritoneal space. By contrast, the murine EFP, and equivalent human omentum, is a highly vascularized and easily manipulated tissue that can enclose delivered islets to create an isolated, retrievable islet graft. Additionally, the omentum is a nonvital organ that can be manipulated laparoscopically, and previous studies support our findings of reduced immune response, despite enhanced islet vascularization, which points to the omentum's superiority over alternative locations (*21*, *27*). These factors, combined with the omentum's high inherent vascularization and advantageous portal drainage (*18*, *47*), support this site's potential

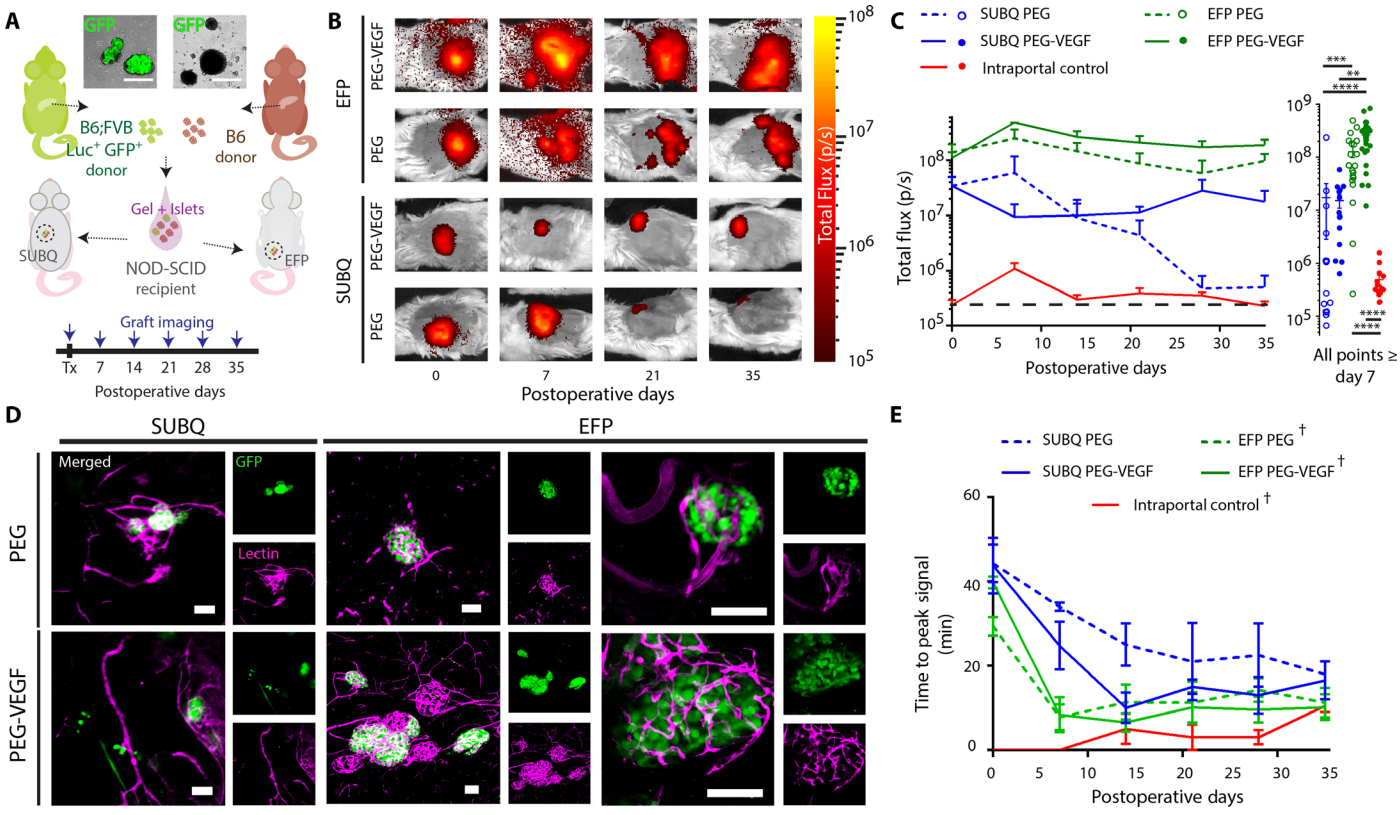

Fig. 5. In vivo bioluminescent islet tracking allows real-time monitoring of islet survival. (**A**) Gels containing Luc$^+$GFP$^+$/B6 hybrid islet grafts, either with or without VEGF, were delivered to extrahepatic sites as demonstrated in the schematic. (**B**) Representative in vivo bioluminescence images. (**C**) Recipients were monitored weekly for bioluminescent signal (left) by intraperitoneal luciferin injection, and cumulative bioluminescent data after day 7 demonstrate significantly enhanced survival in EFP-VEGF group. (**D**) Lectin perfusion at experimental end point allowed visualization of Luc$^+$GFP$^+$/B6 islet graft [GFP (green)] integration with host vasculature [lectin (magenta)]. High-magnification images of EFP/PEG and EFP/PEG-VEGF islets illustrate integration of vasculature with islet organoid structure. (**E**) Time-to-peak bioluminescent signal serves as an additional measure of graft vascularization over time. Error bars represent SEM. $n = 3$ to 4 per group. $^{****}P < 0.0001$, $^{***}P < 0.005$, and $^{**}P < 0.01$, evaluated by Kruskal-Wallis nonparametric tests with Dunn's multiple comparison. $^{\dagger}P < 0.05$ versus SUBQ-PEG, evaluated by one-way ANOVA with repeated measures and Dunnett's multiple comparisons test. Scale bars, 100 μm.

for clinically relevant single pancreatic donor islet mass transplantation. This study highlights that careful consideration of transplant site microenvironments, particularly capacity for vasculogenesis and immune milieu, should inform islet graft transplant site selection in the clinical setting.

Our studies demonstrate that VEGF delivery using this synthetic hydrogel enhances islet survival, vascularization, and function. Early preclinical and clinical models exploring bolus or systemic VEGF delivery demonstrated poor outcomes as a therapeutic effect required large doses and resulted in temporary and leaky/dysfunctional vessels (*48*). In contrast, we and others (*49*–*52*) have shown that sustained VEGF delivery from appropriate biomaterial carriers results in stable, mature, and functional vessels. Furthermore, islets themselves secrete VEGF after transplantation (*53*), supported by our findings of functional organoid vasculature in PEG-only groups within this study.

Islet autotransplantation after total pancreatectomy uses the intrahepatic site for islet mass delivery from a single pancreatic source, and poor outcomes in the absence of the substantial complications of autoimmunity and immune rejection point to the hostility of the hepatic site (*54*). Although the use of syngeneic and immunodeficient mouse models in this study enabled evaluation of islet engraftment and survival in the context of islet autotransplantation after total pancreatectomy, it is unclear how systemic immunosuppression and autoimmunity may contribute to extrahepatic allogeneic islet graft survival and engraftment. The enhanced survival of extrahepatic syngeneic islet grafts observed in our study could translate to greater insulin independence for single pancreatic donor procedures in the context of clinical allogeneic islet transplantation for type 1 diabetes mellitus patients. Further investigations are required to fully elucidate the benefits of extrahepatic allogeneic islet transplantation with the added complexity of autoimmunity and/or systemic immunosuppression. Whereas systemic immunosuppressive agents have been shown to counteract islet revascularization to some degree (*55*), it is possible that this VEGF delivery system may counteract this effect by supplementing native islet VEGF expression and thereby potentially enhance islet revascularization in clinical islet transplantation for type 1 diabetes mellitus patients.

In summary, this study demonstrates that the degree of vascularization of an extrahepatic transplant site in response to a biomaterial vehicle plays a key role in islet engraftment, survival, and function and that VEGF delivery via synthetic hydrogels promotes sufficient engraftment of a single pancreatic donor islet mass to restore nonfasting euglycemia in a syngeneic murine model. These results suggest that islet delivery to the omentum within PEG-VEGF hydrogels may improve rates of insulin independence in patients receiving islet

autotransplantation after pancreatectomy and may greatly reduce the burden on donor organ availability in allogeneic islet transplantation to treat type 1 diabetes mellitus.

MATERIALS AND METHODS

Materials

Chemical reagents were purchased from Sigma-Aldrich, cell culture materials were obtained from Invitrogen, and peptides were synthesized by AAPPTec, unless otherwise noted.

Animals

Animal experiments were performed with the approval of the Georgia Tech Animal Care and Use Committee with veterinary supervision and within the guidelines of the *Guide for the Care and Use of Laboratory Animals*. In syngeneic studies, C57BL/6J male mice (10 to 14 weeks old) were used as recipients, and diabetes was induced by intraperitoneal injection of single-dose streptozotocin (200 mg/kg) on preoperative day 5. C57BL/6J female mice (10 to 14 weeks old) were used as islet donors. For the luciferase islet study, B6;FVB-Ptprc^{a} Tg(CAG-luc,-GFP)L2G85Chco Thy1^{a}/J female mice (8 to 12 weeks old) were used as donors. NOD-SCID male mice (10 to 14 weeks old) were used as recipients, and diabetes was induced by single-dose streptozotocin injection (180 mg/kg) on preoperative day 5. All mice were obtained from the Jackson Laboratory.

Vasculogenic hydrogels

A sterile 5% (final, w/v) solution of a four-arm PEG-maleimide monomer (20 kDa; Laysan Bio) was functionalized with 1.0 mM RGD peptide and VEGF (10 μg/ml) (where applicable) at 37°C for a minimum period of 15 min in gel buffer [phosphate-buffered saline (PBS), 25 mM Hepes; CellGro]. A separate cross-linking solution of VPM peptide was prepared in gel buffer. The pH for all solutions was adjusted to 7.0 to 7.5. To generate gels, functional macromers were rapidly mixed with VPM cross-linker at the site of transplant. The peptide sequences are GCRDVPMSMRGGDRCG for VPM and GRGDSPC for RGD.

Vascularization analyses

For SUBQ grafts, a small incision was made and sufficient connective tissue was cleared to accommodate a 50-μl gel, and the PEG-RGD and VPM cross-linking components were mixed in situ and allowed to polymerize for 10 min before closure with wound clips. For SBM grafts, a small amount of mesentery adjacent to the cecum was exposed. SBM location was chosen to avoid proximity to pancreatic tissue and for ease of graft location postoperatively. EFP tissue was gently exteriorized on a sterile gauze and spread with saline. Gel components were mixed directly on the surface of the SBM or EFP and allowed to cross-link for 10 min before reinsertion into the peritoneal space. For lectin perfusion, anesthetized mice were given an intravenous lectin injection (200 μl; DyLight 488–labeled lectin, Vector Laboratories) and sacrificed after 15 min; the vasculature was flushed with saline before graft removal and fixation in 10% buffered formalin. Grafts were stabilized between glass slides before whole mount–imaging on a confocal microscope. *Z* stacks of each sample were acquired at 4 to 6 FOV, within five to seven grafts per group. Vascular characteristics were analyzed using ImageJ/FIJI and were calculated to obtain an FOV of 1.59×10^{6} μm^{2} (objective, 10×; numerical aperture, 0.3).

Islet engraftment and function in extrahepatic transplant sites

Islets were isolated by pancreatic perfusion with Liberase TL (Roche), for 10 min of digestion at 37°C with gentle shaking and ultrapure (80 to 90%) islet separation from acinar using standard Ficoll gradients (1.108, 1.096, 1.069, and 1.037; Mercodia). Islets were counted using the standard IEQ method and dithizone staining. Two to 3 days after isolation, 600 IEQs were aliquoted in 10 μl of medium and mixed with PEG-RGD gel component just before in situ gelation at the site of transplant. Transplant recipients were monitored for nonfasting blood glucose levels. An IPGTT was performed before sacrifice. At sacrifice, graft recipients were lectin-perfused, as described above. Grafts were additionally stained for insulin (DAKO) using traditional histological techniques with incubation times for permeabilization [Triton X-100 (1 μl/ml) in PBS], blocking (goat serum; BioGenex), and antibody staining extended to 24 hours each to allow whole-graft infiltration.

Histological evaluation

Formalin-fixed grafts were paraffin-embedded and sectioned for staining. Standard antigen retrieval in citrate buffer was used before sequential blocking with Power Block (BioGenex) and goat serum (BioGenex). Primary antibodies (CD31, Thermo Scientific; CD11b, Novus Biologicals; CD45, BioLegend; insulin, DAKO) and isotype control antibodies were incubated overnight at 4°C, and secondary antibodies (Invitrogen) were incubated for 2 hours at room temperature with DAPI before mounting. Quantification of markers was performed using FIJI, where CD11b and CD45 staining was evaluated in four to seven subjects per group, where a minimum of three images per subject were averaged.

In vivo islet tracking

Islets were isolated from B6;FVB Luc^{+}GFP^{+} transgenic (200 IEQs per recipient) and wild-type C57BL/6J mice (400 IEQs per recipient) and transplanted in the SUBQ and EFP sites of NOD-SCID or C57BL/6J recipients. Because of an incomplete backcross in the B6;FVB Luc^{+}GFP^{+} transgenic strain, as well as the expression of xenogeneic GFP and luciferase proteins, NOD-SCID recipients were used to prevent islet rejection. Intraportal islets were slowly infused using 200 μl of saline through the duodenum mesenteric vein, which drains to the hepatic portal vein. Bioluminescence was detected by kinetic monitoring of signal (3-min intervals) after beetle luciferin (Promega) injection under anesthesia, until peak signal was reached, on an IVIS SpectrumCT (PerkinElmer) every week until the end point of the study. Hyperglycemic mice received 4 U of insulin (NovoLog) before imaging. Total flux per graft was measured over a 2-cm-diameter circular region of interest drawn around each graft for quantitative measurements. At sacrifice, graft recipients were lectin-perfused (200 μl; DyLight 649–labeled lectin, Vector Laboratories), as described above, with the exception of formalin fixation. Grafts were placed in saline on ice for immediate whole-mount imaging by confocal microscopy to preserve native GFP expression.

Statistics

All statistical analyses were performed in Prism software (GraphPad). Vascularization metrics, blood glucose data (temporal, >15 day average, and IPGTT), body weights, and bioluminescence data are presented as means ± SEM. For characterization of vascularization metrics, leukocyte quantification, and bioluminescence quantification,

Kruskal-Wallis nonparametric tests with Dunn's multiple comparison of select groups were used for all analyses. Nonparametric two-tailed Spearman correlation analysis for CD11b and CD45 markers plotted against vascular fractional area. Syngeneic blood glucose averages (>15 day) were analyzed by one-way ANOVA. Blood glucose comparison between EFP/PEG-VEGF and intraportal graft performance by two-tailed unpaired *t* test. Time-to-peak curves were analyzed by one-way ANOVA with repeated measures and by Dunnett's multiple-comparisons test against SUBQ/PEG. Survival curve analysis was performed using log-rank (Mantel-Cox) test.

SUPPLEMENTARY MATERIALS

Supplementary material for this article is available at http://advances.sciencemag.org/cgi/content/full/3/6/e1700184/DC1

fig. S1. Gross morphology of extrahepatic transplant sites during gel casting.
fig. S2. Correlation between site vascularization fractional area and site leukocyte density.
fig. S3. Blood glucose traces demonstrating individual recipient graft performance in extrahepatic islet transplant sites.
fig. S4. Long-term engraftment of marginal islet mass in EFP with PEG-VEGF.
fig. S5. Comparison of reversal in intraportal control islet transplant site and EFP/PEG-VEGF transplant site syngeneic diabetes reversal.
fig. S6. Survival curve for SUBQ groups.
fig. S7. Density of vascularized islets by site as demonstrated by lectin labeling.
fig. S8. Dose-dependent response of $Luc^{+}GFP^{+}$ islet signal in B6 recipients in EFP site over a 3-week period.
fig. S9. In vivo imaging of intraportally infused islets.
fig. S10. Bioluminescence signal kinetics by time point.
table S1. Exact *P* values for select comparisons between groups in vascularization metrics analyses.
table S2. Exact *P* values for select comparisons between groups in leukocyte presence analyses.

REFERENCES AND NOTES

1. S. Wild, G. Roglic, A. Green, R. Sicree, H. King, Global prevalence of diabetes estimates for the year 2000 and projections for 2030. *Diabetes Care* **27**, 1047–1053 (2004).
2. Center for Disease Control, "National diabetes fact sheet: National estimates and general information on diabetes and prediabetes in the United States, 2011" (CDC, 2011); https://www.cdc.gov/diabetes/pubs/pdf/ndfs_2011.pdf.
3. R. Calafiore, Perspectives in pancreatic and islet cell transplantation for the therapy of IDDM. *Diabetes Care* **20**, 889–896 (1997).
4. A. Bruni, B. Gala-Lopez, A. R. Pepper, N. S. Abualhassan, A. J. Shapiro, Islet cell transplantation for the treatment of type 1 diabetes: Recent advances and future challenges. *Diabetes Metab. Syndr. Obes. Target Ther.* **7**, 211 (2014).
5. M. D. Bellin, D. E. Sutherland, R. P. Robertson, Pancreatectomy and autologous islet transplantation for painful chronic pancreatitis: Indications and outcomes. *Hosp. Pract.* **40**, 80–87 (2012).
6. A. Balamurugan, T. L. Pruett, Trying to prevent the clogged drain: Optimizing the yield and function of portal vein-infused islets. *Dig. Dis. Sci.* **58**, 1170–1172 (2013).
7. D. B. Kaufman, P. F. Gores, M. J. Field, A. C. Farney, S. A. Gruber, E. Stephanian, D. E. R. Sutherland, Effect of 15-deoxyspergualin on immediate function and long-term survival of transplanted islets in murine recipients of a marginal islet mass. *Diabetes* **43**, 778–783 (1994).
8. R. Bottino, L. A. Fernandez, C. Ricordi, R. Lehmann, M.-F. Tsan, R. Oliver, L. Inverardi, Transplantation of allogeneic islets of Langerhans in the rat liver: Effects of macrophage depletion on graft survival and microenvironment activation. *Diabetes* **47**, 316–323 (1998).
9. N. S. Kenyon, L. A. Fernandez, R. Lehmann, M. Masetti, A. Ranuncoli, M. Chatzipetrou, G. Iaria, D. Han, J. L. Wagner, P. Ruiz, M. Berho, L. Inverardi, R. Alejandro, D. H. Mintz, A. D. Kirk, D. M. Harlan, L. C. Burkly, C. Ricordi, Long-term survival and function of intrahepatic islet allografts in baboons treated with humanized anti-CD154. *Diabetes* **48**, 1473–1481 (1999).
10. M. Biarnés, M. Montolio, V. Nacher, M. Raurell, J. Soler, E. Montanya, β-Cell death and mass in syngeneically transplanted islets exposed to short-and long-term hyperglycemia. *Diabetes* **51**, 66–72 (2002).
11. F. B. Barton, M. R. Rickels, R. Alejandro, B. J. Hering, S. Wease, B. Naziruddin, J. Oberholzer, J. S. Odorico, M. R. Garfinkel, M. Levy, F. Pattou, T. Berney, A. Secchi, S. Messinger, P. A. Senior, P. Maffi, A. Posselt, P. G. Stock, D. B. Kaufman, X. Luo, F. Kandeel, E. Cagliero, N. A. Turgeon, P. Witkowski, A. Naji, P. J. O'Connell, C. Greenbaum, Y. C. Kudva, K. L. Brayman, M. J. Aull, C. Larsen, T. W. H. Kay, L. A. Fernandez, M.-C. Vantyghem, M. Bellin, A. M. J. Shapiro, Improvement in outcomes of clinical islet transplantation: 1999–2010. *Diabetes Care* **35**, 1436–1445 (2012).
12. A. R. Pepper, B. Gala-Lopez, R. Pawlick, S. Merani, T. Kin, A. M. J. Shapiro, A prevascularized subcutaneous device-less site for islet and cellular transplantation. *Nat. Biotechnol.* **33**, 518–523 (2015).
13. S. Veriter, P. Gianello, Y. Igarashi, G. Beaurin, A. Ghyselinck, N. Aouassar, B. Jordan, B. Gallez, D. Dufrane, Improvement of subcutaneous bioartificial pancreas vascularization and function by coencapsulation of pig islets and mesenchymal stem cells in primates. *Cell Transplant.* **23**, 1349–1364 (2014).
14. M. S. Kim, H. H. Ahn, Y. N. Shin, M. H. Cho, G. Khang, H. B. Lee, An in vivo study of the host tissue response to subcutaneous implantation of PLGA-and/or porcine small intestinal submucosa-based scaffolds. *Biomaterials* **28**, 5137–5143 (2007).
15. A. Pileggi, R. D. Molano, C. Ricordi, E. Zahr, J. Collins, R. Valdes, L. Inverardi, Reversal of diabetes by pancreatic islet transplantation into a subcutaneous, neovascularized device. *Transplantation* **81**, 1318–1324 (2006).
16. C. B. Kemp, M. J. Knight, D. W. Scharp, W. F. Ballinger, P. E. Lacy, Effect of transplantation site on the results of pancreatic islet isografts in diabetic rats. *Diabetologia* **9**, 486–491 (1973).
17. E. A. Phelps, D. M. Headen, W. R. Taylor, P. M. Thule, A. J. García, Vasculogenic bio-synthetic hydrogel for enhancement of pancreatic islet engraftment and function in type 1 diabetes. *Biomaterials* **34**, 4602–4611 (2013).
18. A. O. Gaber, A. Chamsuddin, D. Fraga, J. Fisher, A. Lo, Insulin independence achieved using the transmesenteric approach to the portal vein for islet transplantation. *Transplantation* **77**, 309–311 (2004).
19. T. Kin, G. S. Korbutt, R. V. Rajotte, Survival and metabolic function of syngeneic rat islet grafts transplanted in the omental pouch. *Am. J. Transplant.* **3**, 281–285 (2003).
20. Y. Yasunami, P. E. Lacy, E. H. Finke, A new site for islet transplantation—A peritoneal-omental pouch. *Transplantation* **36**, 181–182 (1983).
21. S. Merani, C. Toso, J. Emamaullee, A. M. J. Shapiro, Optimal implantation site for pancreatic islet transplantation. *Br. J. Surg.* **95**, 1449–1461 (2008).
22. D. M. Berman, J. J. O'Neil, L. C. K. Coffey, P. C. J. Chaffanjon, N. M. Kenyon, P. Ruiz Jr., A. Pileggi, C. Ricordi, N. S. Kenyon, Long-term survival of nonhuman primate islets implanted in an omental pouch on a biodegradable scaffold. *Am. J. Transplant.* **9**, 91–104 (2009).
23. X. Chen, X. Zhang, C. Larson, F. Chen, H. Kissler, D. B. Kaufman, The epididymal fat pad as a transplant site for minimal islet mass. *Transplantation* **84**, 122–125 (2007).
24. A.-C. Brady, M. M. Martino, E. Pedraza, S. Sukert, A. Pileggi, C. Ricordi, J. A. Hubbell, C. L. Stabler, Proangiogenic hydrogels within macroporous scaffolds enhance islet engraftment in an extrahepatic site. *Tissue Eng. Part A* **19**, 2544–2552 (2013).
25. C. E. Brubaker, H. Kissler, L.-J. Wang, D. B. Kaufman, P. B. Messersmith, Biological performance of mussel-inspired adhesive in extrahepatic islet transplantation. *Biomaterials* **31**, 420–427 (2010).
26. A. Rajab, Islet transplantation: Alternative sites. *Curr. Diab. Rep.* **10**, 332–337 (2010).
27. D. J. van der Windt, G. J. Echeverri, J. N. Ijzermans, D. K. C. Cooper, The choice of anatomical site for islet transplantation. *Cell Transplant.* **17**, 1005–1014 (2008).
28. R. P. Robertson, Islet transplantation as a treatment for diabetes—A work in progress. *N. Engl. J. Med.* **350**, 694–705 (2004).
29. A. Andersson, O. Korsgren, L. Jansson, Intraportally transplanted pancreatic islets revascularized from hepatic arterial system. *Diabetes* **38** suppl. 1, 192–195 (1989).
30. T. K. Hart, R. M. Pino, Pseudoislet vascularization. Induction of diaphragm-fenestrated endothelia from the hepatic sinusoids. *Lab. Invest.* **54**, 304–313 (1986).
31. M. Brissova, A. C. Powers, Revascularization of transplanted islets: Can it be improved? *Diabetes* **57**, 2269–2271 (2008).
32. P.-O. Carlsson, F. Palm, A. Andersson, P. Liss, Markedly decreased oxygen tension in transplanted rat pancreatic islets irrespective of the implantation site. *Diabetes* **50**, 489–495 (2001).
33. G. Mattsson, L. Jansson, P.-O. Carlsson, Decreased vascular density in mouse pancreatic islets after transplantation. *Diabetes* **51**, 1362–1366 (2002).
34. N. R. Barshes, S. Wyllie, J. A. Goss, Inflammation-mediated dysfunction and apoptosis in pancreatic islet transplantation: Implications for intrahepatic grafts. *J. Leukoc. Biol.* **77**, 587–597 (2005).
35. J. A. Emamaullee, A. M. J. Shapiro, Factors influencing the loss of β-cell mass in islet transplantation. *Cell Transplant.* **16**, 1–8 (2007).
36. T. Linn, J. Schmitz, I. Hauck-Schmalenberger, Y. Lai, R. G. Bretzel, H. Brandhorst, D. Brandhorst, Ischaemia is linked to inflammation and induction of angiogenesis in pancreatic islets. *Clin. Exp. Immunol.* **144**, 179–187 (2006).
37. K. Cheng, D. Fraga, C. Zhang, M. Kotb, A. O. Gaber, R. V. Guntaka, R. I. Mahato, Adenovirus-based vascular endothelial growth factor gene delivery to human pancreatic islets. *Gene Ther.* **11**, 1105–1116 (2004).
38. A. S. Narang, K. Cheng, J. Henry, C. Zhang, O. Sabek, D. Fraga, M. Kotb, A. O. Gaber, R. I. Mahato, Vascular endothelial growth factor gene delivery for revascularization in transplanted human islets. *Pharm. Res.* **21**, 15–25 (2004).

39. S. Sigrist, A. Mechine-Neuville, K. Mandes, V. Calenda, S. Braun, G. Legeay, J.-P. Bellocq, M. Pinget, L. Kessler, Influence of VEGF on the viability of encapsulated pancreatic rat islets after transplantation in diabetic mice. *Cell Transplant.* **12**, 627–635 (2003).
40. N. Zhang, A. Richter, J. Suriawinata, S. Harbaran, J. Altomonte, L. Cong, H. Zhang, K. Song, M. Meseck, J. Bromberg, H. Dong, Elevated vascular endothelial growth factor production in islets improves islet graft vascularization. *Diabetes* **53**, 963–970 (2004).
41. J. C. Stendahl, L.-J. Wang, L. W. Chow, D. B. Kaufman, S. I. Stupp, Growth factor delivery from self-assembling nanofibers to facilitate islet transplantation. *Transplantation* **86**, 478–481 (2008).
42. M. Najjar, V. Manzoli, M. Abreu, C. Villa, M. M. Martino, R. D. Molano, Y. Torrente, A. Pileggi, L. Inverardi, C. Ricordi, J. A. Hubbell, A. A. Tomei, Fibrin gels engineered with pro-angiogenic growth factors promote engraftment of pancreatic islets in extrahepatic sites in mice. *Biotechnol. Bioeng.* **112**, 1916–1926 (2015).
43. E. A. Phelps, N. O. Enemchukwu, V. F. Fiore, J. C. Sy, N. Murthy, T. A. Sulchek, T. H. Barker, A. J. García, Maleimide cross-linked bioactive PEG hydrogel exhibits improved reaction kinetics and cross-linking for cell encapsulation and in situ delivery. *Adv. Mater.* **24**, 64–70 (2012).
44. B. Nilsson, O. Korsgren, J. D. Lambris, K. N. Ekdahl, Can cells and biomaterials in therapeutic medicine be shielded from innate immune recognition? *Trends Immunol.* **31**, 32–38 (2010).
45. W. Bennet, C.-G. Groth, R. Larsson, B. Nilsson, O. Korsgren, Isolated human islets trigger an instant blood mediated inflammatory reaction: Implications for intraportal islet transplantation as a treatment for patients with type 1 diabetes. *Ups. J. Med. Sci.* **105**, 125–133 (2000).
46. O. Korsgren, T. Lundgren, M. Felldin, A. Foss, B. Isaksson, J. Permert, N. H. Persson, E. Rafael, M. Rydén, K. Salmela, A. Tibell, G. Tufveson, B. Nilsson, Optimising islet engraftment is critical for successful clinical islet transplantation. *Diabetologia* **51**, 227–232 (2008).
47. A. O. Gaber, M. H. Shokouh-Amiri, D. K. Hathaway, L. Hammontree, A. E. Kitabchi, L. W. Gaber, M. F. Saad, L. G. Britt, Results of pancreas transplantation with portal venous and enteric drainage. *Ann. Surg.* **221**, 613–624 (1995).
48. A. Pettersson, J. A. Nagy, L. F. Brown, C. Sundberg, E. Morgan, S. Jungles, R. Carter, J. E. Krieger, E. J. Manseau, V. S. Harvey, I. A. Eckelhoefer, D. Feng, A. M. Dvorak, R. C. Mulligan, H. F. Dvorak, Heterogeneity of the angiogenic response induced in different normal adult tissues by vascular permeability factor/vascular endothelial growth factor. *Lab. Invest.* **80**, 99–115 (2000).
49. M. Ehrbar, S. M. Zeisberger, G. P. Raeber, J. A. Hubbell, C. Schnell, A. H. Zisch, The role of actively released fibrin-conjugated VEGF for *VEGF receptor 2* gene activation and the enhancement of angiogenesis. *Biomaterials* **29**, 1720–1729 (2008).
50. W. M. Elbjeirami, J. L. West, Angiogenesis-like activity of endothelial cells co-cultured with VEGF-producing smooth muscle cells. *Tissue Eng. Part A* **12**, 381–390 (2006).
51. V. Sacchi, R. Mittermayr, J. Hartinger, M. M. Martino, K. M. Lorentz, S. Wolbank, A. Hofmann, R. A. Largo, J. S. Marschall, E. Groppa, R. Gianni-Barrera, M. Ehrbar, J. A. Hubbell, H. Redl, A. Banfi, Long-lasting fibrin matrices ensure stable and functional angiogenesis by highly tunable, sustained delivery of recombinant $VEGF_{164}$. *Proc. Natl. Acad. Sci. U.S.A.* **111**, 6952–6957 (2014).
52. E. A. Phelps, N. Landázuri, P. M. Thulé, W. R. Taylor, A. J. García, Bioartificial matrices for therapeutic vascularization. *Proc. Natl. Acad. Sci. U.S.A.* **107**, 3323–3328 (2010).
53. M. Brissova, A. Shostak, M. Shiota, P. O. Wiebe, G. Poffenberger, J. Kantz, Z. Chen, C. Carr, W. G. Jerome, J. Chen, H. S. Baldwin, W. Nicholson, D. M. Bader, T. Jetton, M. Gannon, A. C. Powers, Pancreatic islet production of vascular endothelial growth factor-A is essential for islet vascularization, revascularization, and function. *Diabetes* **55**, 2974–2985 (2006).
54. K. Bramis, A. N. Gordon-Weeks, P. J. Friend, E. Bastin, A. Burls, M. A. Silva, A. R. Dennison, Systematic review of total pancreatectomy and islet autotransplantation for chronic pancreatitis. *Br. J. Surg.* **99**, 761–766 (2012).
55. M. D. Menger, J.-i. Yamauchi, B. Vollmar, Revascularization and microcirculation of freely grafted islets of Langerhans. *World J. Surg.* **25**, 509–515 (2001).

Acknowledgments

Funding: This research was supported by the Juvenile Diabetes Research Foundation (grant 2-SRA-2014-287-Q-R to A.J.G., H.S., and L.D.S.), the NIH Innovation and Leadership in Engineering Technologies and Therapies Postdoctoral Training (grant T90-DK097787-03 to J.D.W.), and the Ruth L. Kirschstein National Research Service Award (F30AR069472) from the National Institute of Arthritis and Musculoskeletal and Skin Diseases (to C.T.J.). **Author contributions:** J.D.W. and A.J.G. designed the experiments; J.D.W., D.M.H., J.A., and C.T.J. performed the experiments; J.D.W., A.J.G., L.D.S., H.S., and D.M.H. discussed the results; J.D.W. prepared the figures; and J.D.W. and A.J.G. prepared the manuscript. **Competing interests:** H.S. is Founder and CEO of FasCure Therapeutics LLC. All other authors declare that they have no competing interests. **Data and materials availability:** All data needed to evaluate the conclusions in the paper are present in the paper and/or the Supplementary Materials. Additional data related to this paper may be requested from the authors.

Submitted 17 January 2017
Accepted 3 April 2017
Published 2 June 2017
10.1126/sciadv.1700184

Citation: J. D. Weaver, D. M. Headen, J. Aquart, C. T. Johnson, L. D. Shea, H. Shirwan, A. J. García, Vasculogenic hydrogel enhances islet survival, engraftment, and function in leading extrahepatic sites. *Sci. Adv.* **3**, e1700184 (2017).